Characterizing the Sphingomyelinase Pathway Triggered by PRIMA-1 Derivatives in Lung Cancer Cells with Differing p53 Status

EROICA SOANS[1], SUSAN C. EVANS[2], CYNTHIA CIPOLLA[3*] and ELROY FERNANDES[4**]

[1,2,3,4]*Department of Chemistry and Biochemistry, Konneker Research Laboratories, Ohio University, The Ridges-Ohio University, Athens, OH, U.S.A.*

Abstract. *Background/Aim: Derivatives of PRIMA-1 compound, 8a and 8b have been shown to increase cytotoxicity in lung cancer cells through sphingomyelinase pathways in IR and 8a or 8b co-treated lung cancer cells. The goal of the present study was to further elaborate the molecular mechanism of 8a- or 8b-treated lung cancer cells in order to understand their potential as anti-cancer drugs. Materials and Methods: Biochemical assays, western blot, flow cytometry and gene array analyses were employed to distinguish these mechanisms. Results: Herein we demonstrated that 8a and 8b cause apoptosis with S-phase arrest in lung cancer cells by activating neutral sphingomyelinase with ceramide production. 8a induces expression of TNF family genes while 8b induces p53-mediated apoptosis genes. Protein analysis shows an increased expression in caspase 8, bcl-2, bax, caspase 9 and cytochrome c. Conclusion: PRIMA-1 derivatives provoke cytotoxicity in lung cancer cells mainly through the neutral sphingomyelinase-dependent apoptosis pathway.*

PRIMA-1 (p53 reactivation and induction of massive apoptosis) is a low molecular weight compound 2, 2-bis (hydroxymethyl)-1-azabicyclo [2,2,2] octan-3-one. It restores mutant p53 activity in cell lines expressing His 175 mutant p53. This mutation causes major structural defect, as wild-type Arg 175 is required for stabilizing the DNA binding domain structure and is frequently mutated and linked to improper protein folding. PRIMA-1 acts by forming adducts with the thiols present on p53 through covalent modification, allowing for the correct folding of the p53 protein so that it can bind DNA and transactivate downstream genes (1-4).

PRIMA-1 is shown to increase the promoter activity and protein expression of bax and PUMA, known transcriptional targets of p53, and lower the expression of c-Jun and phosphorylated c-Jun suggesting that PRIMA-1 causes apoptosis through bax and PUMA but not JNK signaling (5). In NSCLC cells expressing the *His 175* mutation and colon cancers with mutant *p53*, PRIMA-1 caused G_2 arrest with up-regulation in p21 and Gadd45a proteins (known transcriptional targets of p53) along with the induction of JNK signaling pathway, but did not have any effect on Fas, bcl-2 related proteins, caspase 8, caspase 9 or caspase 3 (6). Taken together these studies suggest that PRIMA-1 molecular mechanisms are cell type dependent. In 2006, Malki *et al.* showed using MTT assay that detects mitochondrial activity in viable cells that derivatives of PRIMA-1, 8a or 8b showed better activity than the lead compound in NSCLC cell lines than normal lung epithelial cells (7).

In 2011, Malki *et al.* suggested that quinuclidinone derivatives 8a and 8b cause apoptosis by activating sphingomyelinase and they are radio sensitizers that abrogate G_2-M phase by activating p53 and caspase-3 in IR-8a and IR-8b treated cells (8).

The goal of the present study was to understand the mechanism of action of quinuclidinone derivatives that activate sphingomyelinase to further understand the increased anticancer potential of 8a and 8b. Herein we demonstrated that 8a and 8b cause apoptosis in H1299 and H1299p53+/+ cell lines with S-phase cell-cycle arrest. Importantly 8a activates sphingomyelinase primarily neutral

**Present address:* Department of Chemistry, University of Michigan, 930N University, Ann Arbor, MI 48109

***Present address:* Department of Clinical Research Administration, St Jude Children's Research Hospital, 262 Danny Thomas Pl, Memphis, TN 38105

Correspondence to: Eroica Soans, Current Address: Department of Pathology, St Jude Children's Research Hospital, 262 Danny Thomas Pl, Memphis, TN 38105, U.S.A. Tel: +1 9015956410, Fax: +1 9015955947, e-mail: eroica.soans@stjude.org

Key Words: Sphingomyelinase, p53, PRIMA-1, lung cancer, apoptosis.

sphingomyelinase (N-SMase) than acid sphingomyelinase (A-SMase) in H1299 cells and to a much lower extent only A-SMase in H1299 cells transfected with p53. While 8b activates mainly N-SMase rather than A-SMase in both cell lines. Ceramide production is mainly due to sphingomyelinase and not due to ceramide synthase in cells treated with 8a and 8b. Gene expression arrays analysis showed that 8a mainly induces expression of genes belonging to the TNF family while 8b induces expression of genes belonging to the p53 mediated apoptosis pathway and inhibits gene expression of inhibitors of the pathway. Caspase 8, bcl-2, bax, caspase 9, cytochrome *c* protein expression analysis indicate their role in neutral sphingomyelinase-mediated apoptosis.

Materials and Methods

Cell culture. H1299 cells were provided by Jack Roth, M.D. Anderson Cancer Center. H1299 p53+/+ is a stably-transfected cell line generated in the laboratory having wild type p53 activity. The cells were maintained in Dulbecco's Modified Eagle's Medium (DMEM, Hyclone, Utah, USA) supplemented with 10% (v/v) bovine growth serum (Hyclone, Utah, USA) and 1% (v/v) penicillin streptomycin (Hyclone) and incubated in an environment of 95% air and 5% CO_2 at 37˚C. For treatment, quinuclidinone derivatives were prepared in appropriate media using IC_{50} concentration as determined earlier (7).

Chemicals. 8a and 8b were synthesized in the laboratory of Stephen Bergmeier, PhD, Department of Chemistry and Biochemistry, Ohio University. 100 μM concentration of the derivatives were used in the current study based on previous studies (7, 8). Inhibitors used were N-SMase inhibitor GW4869 (15 μM), A-SMase inhibitor desipramine (10 μM) and ceramide synthase inhibitor fumonisin B1 (50 μM) purchased from Sigma (St. Louis, MO, USA).

Apoptosis measurement using caspase-3 activity. Caspase-3 enzyme activity was measured using EnzChek® Caspase-3 assay kit 1 (Molecular Probes INC, Eugene, OR, USA). The cells were treated with 100 μM 8a and 8b for 24 h and assayed according to the manufacturer's protocol. Cells were lysed using Lysis buffer provided in the kit. Supernatant collected after centrifugation was used for the assay as well as for protein estimation as described later. The supernatant was mixed with substrate Z-DEVD-AMC in a 96-well plate. Control without enzyme was assayed for each experiment to determine the background fluorescence. Caspase-3 inhibitor (Ac-DEVD-CHO inhibitor) provided in the kit was added to control wells. Fluorescence was measured at excitation wavelength of 342 nm and emission wavelength of 441 nm. Each experiment was performed in triplicate and statistical significance determined.

Cell-cycle analysis using flow cytometry. Cells were seeded at a density of 3×10^5 in 100-mm plates. Cells were then switched to serum-free media to synchronize the cell cycle. After 24 h, the media were changed to complete media containing 8a or 8b (100 μM). Cells were harvested after 24 h by trypsinization and washed with cold PBS and fixed in ice-cold ethanol (70%) overnight. Finally, the cells were centrifuged and cell pellets were re-suspended in PBS containing 5 μg/mL RNase A (Sigma) and 50 μg/mL propidium iodide (Sigma) for analysis. Cell-cycle analysis was performed using the FACScan Flow Cytometer (Becton Dickson) according to the manufacturer's protocol. The Modfit software was used to calculate the cell-cycle phase distribution from the resultant DNA histogram, and expressed as a percentage of cells in the G_1 (G_0/G_1), S and G_2 (G_2/M) phases. Each assay was performed in triplicate and the standard deviation was determined.

Analysis of sphingomyelinase activity. Sphingomyelinase activity was determined *in vitro* by Amplex Red sphingomyelinase assay (Molecular probes INC, USA) in a 96-well micro-plate reader according to manufacturer's protocol. Briefly, 4,000-5,000 cells/well in 100 μL of medium were seeded in a 96-well plate for 24 h prior to drug treatment. The media was then changed to media with analogs (100 μM). Samples were diluted with reaction buffer and pipetted into 96-well micro-plates. 100 μL of 100 μM Amplex Red reagent containing 2U/ml Horse radish peroxidase (HPR), 0.2 U/ml choline oxidase, 8 U/ml alkaline phosphatase and 0.5 mM sphingomyelin working solution was added to each sample and incubated for 30 min, protected from light. Fluorescence was measured in a fluorescence micro-plate reader (Spectra Max Plus) using excitation range of 530-560 and emission detection at 590 nm. Each experiment was performed in triplicate and standard deviation determined.

Flow cytometry analysis for ceramide production. Cells treated with or without derivatives 8a and 8b (100 μM) were fixed with formaldehyde (final concentration 4% in PBS) for 10 min at 37˚C and then chilled on ice for 1 min. Cells were then permeabilized using ice-cold 90% methanol for 30 min on ice. Permeabilized cells were then washed and re-suspended in PBS and placed in a round-bottomed 96-well plate. They were further incubated for 45 min with mouse monoclonal anti-CER 15B4 (Alexis, Coger, Paris, France). Cells were then washed with PBS containing 0.5% heat-inactivated FBS and incubated for another 30 min with (FITC)-labeled goat anti-mouse (BD Biosciences, San Jose, CA, USA). The cells were washed for a final time with PBS and then subjected to fluorescent activated cell sorter (FACS) analysis (Becton Dickinson) and data was analyzed using CellQuest software.

Cell viability analysis using MTT assay for inhibitor analysis. Cell viability was measured using the methyl tetrazolium (MTT) bromide mitochondrial activity assay (ATCC, Manassas, VA USA) according to the manufacturer's protocol. Cells (at a density of 5-10×10^3 per well) in 100 μL of medium were added to a 96-well plate and incubated for 24 h. The media was then changed to media containing inhibitors and/or 100 μM of derivatives. After 24 h incubation, 10 μL of MTT reagent was added to each well and incubated for 4 h at 37˚C. After incubation, 100 μL of detergent was added to dissolve the formazan crystals and incubated overnight at RT in the dark. The absorbance was then measured at 570 nm. Each assay was performed in triplicate and statistical analysis performed.

Western blot analysis. Total protein was extracted from treated and untreated cells using lysis buffer (10 mM Tris HCl pH 7.5, 1 mM EDTA, 1% triton X-100, 150 mM NaCl, 1 mM dithiothretol, 10% glycerol, 0.2 mM phenylmethylsulphonyl fluoride and protease

inhibitors) for 30-50 min on ice. The extracts were centrifuged at 13,000 rpm for 15 min at 4˚C to remove cell debris. Folin Lowry (Pierce, Thermo Fisher Scientific, Rockford, IL, USA) protein assay was used to determine the protein concentration in the cell lysates. Proteins were resolved by electrophoresis on 8-10% sodium dodecyl sulphate – polyacrylamide gel. The resolved proteins were transferred onto PVDF membrane and then probed with primary antibody against the protein of interest prepared in 5% milk/PBS-T. The membrane was washed using PBS-T and then appropriate secondary antibody conjugated to HRP was used for visualization of the bands using ECL chemiluminescence kit (GE Healthcare Bio-Sciences, Pittsburgh, PA, USA). Anti-caspase-8, anti-bax, anti-caspase 9, anti-BCL-2, anti-procaspase 3 and anti-PARP-1 were purchased from SantaCruz Biotechnology INC, Dallas, TX, USA. Pixel density of the proteins studied was calculated using Image J, version 1.41o, NIH. The values obtained were first normalized to loading control (GAPDH/β-actin) and fold increase was measured by normalizing to the control (0 h) value. At least two or more independent experiments were performed.

Mitochondria and cytosol protein isolation using differential centrifugation for detection of cytochrome c. H1299 and H1299 p53 +/+ cells were treated with 100 μM quinuclidinone derivative 8a and 8b or left untreated for 24 h. After treatment the cells were washed with ice-cold 1X PBS containing 1 mM phenylmethylsulphonyl fluoride (PMSF) and resuspended in 1 mL isolation buffer pH 7.5 (250 mM sucrose, 10 mM HEPES, 1mM EDTA, 10 μl of proteinase inhibitors cocktail and 1 mM PMSF). After 20 min incubation on ice, the suspensions were dounced (3-4 times), checked for lysis with trypan blue then the nuclei and unbroken cells were pelleted by centrifugation at 500 × *g* for 10 min at 4˚C. The supernatants were re-centrifuged at 500 × *g* for 10 min at 4˚C to remove any residual nuclei or unbroken cells. The supernatants were then centrifuged at 7900 × *g* for 10 min at 4˚C to pellet the mitochondria which were resuspended in 200 μl isolation buffer and the resultant supernatant was designated as the cytosolic fraction. 50 μg of both the mitochondrial and cytosolic proteins were then western blotted using anti-cytochrome c antibody from Santa Cruz Biotechnology.

Apoptosis gene array analysis using real-time RT-PCR. Treated and untreated cells were subjected to total RNA extraction using RNeasy Total RNA extraction kit (Qiagen, Inc.; Valencia, CA, USA). Before preparing the cDNA, the quality of RNA isolated was evaluated using Human RT RNA QC PCR Array (SABiosciences; Frederick, MD, USA) then reverse transcription polymerase chain reaction (RT-PCR) was performed on 1 μg of respective total RNA using RT2 First Strand Kit (SABiosciences). The cDNA were mixed with RT. qPCR Master Mixes (SABiosciences) according to the manufacturer's protocol and then aliquoted to the Human Apoptosis RT Profiler™ PCR Array (SABiosciences) containing 84 relevant apoptosis genes and 5 housekeeping genes (Glyceraldehyde-3-phosphate dehydrogenase (*GAPDH*), *β-actin*, Hypoxanthine phosphoribosyl transferase 1 (*HPRT1*), Ribosomal protein L13a (*RPL13A*), β-2-microglobulin (*B2M*)) primer sets, RNA transcription controls, genomic DNA control and positive PCR controls on a 96-well plate. The PCR reaction was performed in Bio-Rad iCycler (Bio-Rad; Hercules, CA, USA) and fold change in expression levels of the genes under study was calculated using ΔΔCt method. Ribosomal protein L13a, GAPDH and β-actin were used as internal control for normalization.

Statistical analysis. All data were analyzed by student *t*-test and expressed as mean±standard deviation. A *p*-value of less than 0.05 was considered statistically significant. Data were obtained from three independent experiments each executed in triplicate.

Results

8a and 8b induce caspase 3 activity and cause S phase arrest. Previous reports on quinuclidinone derivatives have shown that 8a/8b along with radiation, induce caspase 3 activity thereby an indicator for apoptosis occurring in lung cancer cells treated with IR and quinuclidinone derivatives. Here we demonstrate the mechanism of quinuclidinone derivatives by themselves as potential chemotherapeutics that activate caspase-3, a known apoptosis effector (9). Herein, the activity of this enzyme in H1299 and H1299 p53+/+ cells treated with 100 μM of 8a and 8b was evaluated. 8a induced caspase 3 activity more significantly ($p<0.01$) than 8b ($p<0.05$) in H1299 cells as compared to its untreated control (Figure 1A). Similarly, 8b significantly ($p<0.05$) increased the enzyme activity in H1299 p53+/+ cells as compared to the untreated control (Figure 1B). Furthermore, procaspase-3 (32 kDa full-length fragment) expression determined by western blot analysis decreased 24 h after treatment with 8a and 8b in H1299 and H1299 p53+/+ cell lines, which corroborates with the activation of caspase-3 enzyme (Figure 1C). PARP-1 repairs DNA damage, but when cleaved by serine protease caspase-3, the activity decreases. 8a induced time dependent processing of PARP-1 in H1299 cells; as the treatment time increased there was decrease in the 116-kDa active form and the inactive cleaved 89 kDa protein increased. While in H1299 p53 +/+ cells treated with 8a, the 116-kDa active form decreased in a time dependent manner but the 89 kDa inactive form did not increased until 6 hr of treatment (Figure 1D). Similarly, 8b induced time-dependent processing of PARP-1 in H1299 cells wherein the 116-kDa active form decreased and the 89-kDa protein inactive form increased with time. However, in H1299 p53+/+ cells there was decrease in the 116 kDa active form at 6 and 24 h treatment with a transient increase at 12 h but a time dependent continuous increase in the 89-kDa inactive form (Figure 1E). However, both 8a and 8b induced maximum processing after 24 h treatment as compared to the untreated control (0 h) in H1299 and H1299 p53+/+ cells correlating with the caspase 3 activity.

To evaluate whether apoptosis stimulation by 8a and 8b was attributed to the changes in cell cycle regulation, we examined the cell-cycle distribution by flow cytometry in H1299 and H1299 p53+/+ cells undergoing apoptosis after treatment for 24 h with derivatives 8a and 8b. An increase of cells in S phase and decrease in G_0/G_1 and G_2/M phases was detected as compared to the untreated cells in both H1299 and H1299 p53+/+ cell lines after treatment with 8a and 8b. 8b treated

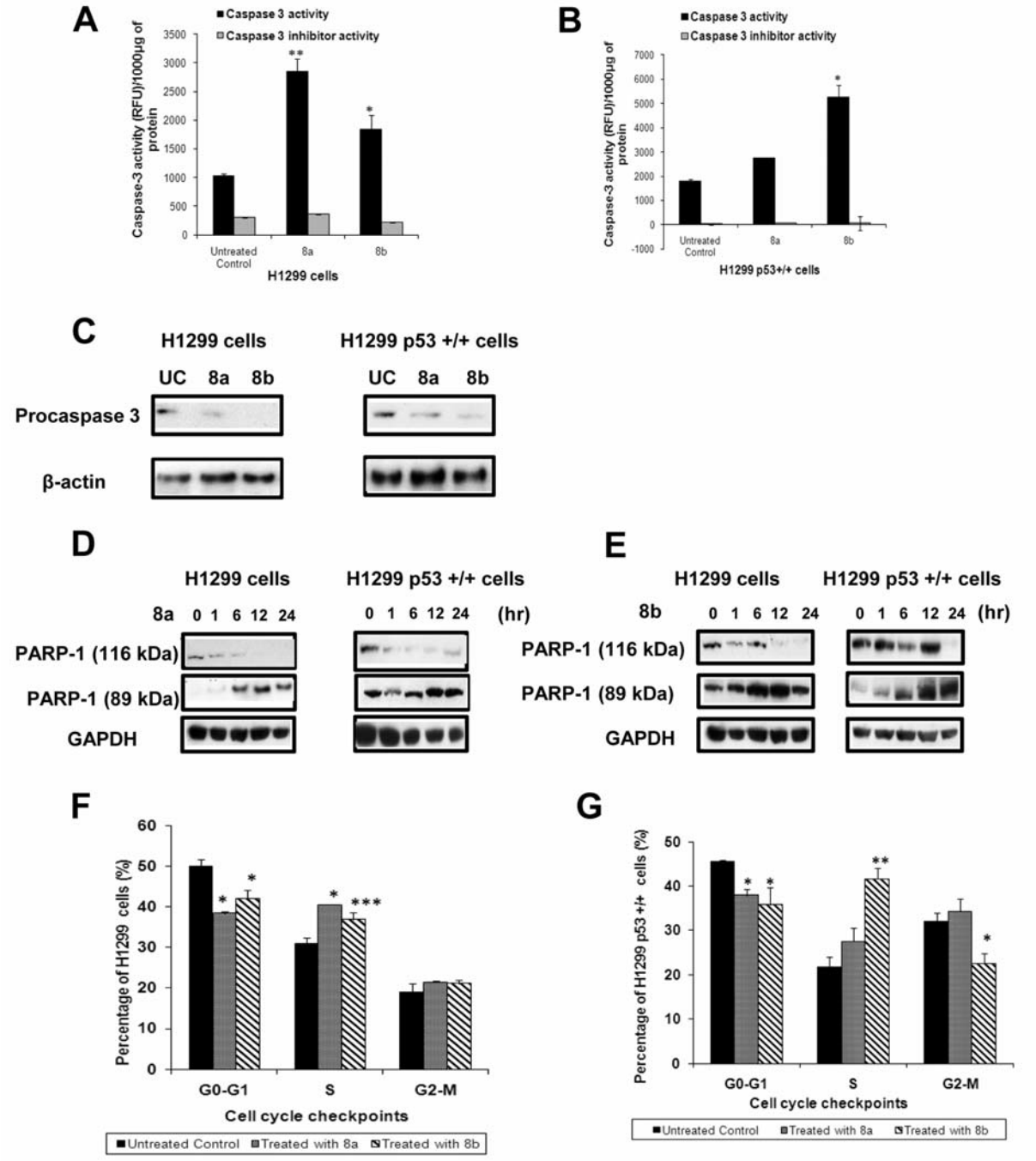

Figure 1. *8a and 8b induce apoptosis and S phase arrest in lung cancer cells. H1299 (A/C) and H1299 p53 +/+ (B/C) cells were treated with 100 µM of 8a and 8b or left untreated (Untreated Control, UC) for 24 hr. Endogenous caspase 3 activity was determined for H1299 (A) and H1299 p53 +/+ (B) cells as described in Materials and Methods and Ac-DEVD-CHO inhibitor was used to indicate the background fluorescence. The histogram represents mean fluorescence (+ SD) measured at excitation/emission 496/520 nm of 3 independent experiments done in triplicate. Significance as compared to the untreated control was * $p < 0.05$ and ** $p < 0.01$. (C) Procaspase 3 levels were determined by western blot analysis using mouse anti-caspase 3 antibody from whole cell lysates and β-actin was used as the loading control. Results are representative of 3 independent experiments. H1299 and H1299 p53 +/+ cells were treated with 100 µM of 8a (D) and 8b (E) for indicated time intervals. PARP-1 cleavage was determined by western blot analysis using mouse anti-PARP-1 antibody from whole cell lysates that detects the 116 kDa full-length and 89 kDa cleavage product. GAPDH was used as the loading control. Results are representative of 3 independent experiments. H1299 (F) and H1299 p53 +/+ (G) cells were treated with 100 µM of 8a and 8b or left untreated (Untreated Control) for 24 hr and analyzed by flow cytometry for cell cycle distribution analysis as described in Materials and Methods. The histogram represents mean percentage of cells (+ SD) in different phases as analyzed using Modfit software of 3 independent experiments. Significance as compared to the untreated control was * $p < 0.05$, ** $p < 0.01$ and *** $p < 0.001$.*

H1299 p53+/+ cells demonstrated a more significant S phase arrest than 8a treated cells; while in H1299 cells both derivatives had similar trends (Figure 1F and G).

Mechanistic studies evaluating the role of sphingomyelinase in 8a and 8b mediated cytotoxicity. After establishing, derivatives 8a and 8b alone can also cause apoptosis and alter cell-cycle progression in human lung cancer cells. Sphingomyelin pathway has been implicated in 8a and 8b based apoptosis (8) but its role in 8a and 8b induced cytotoxic effect has not been shown; sphingomyelinase enzyme is involved in the catabolism of sphingomyelin present in the plasma membrane to produce ceramide, an important second messenger triggering downstream apoptotic targets. We next evaluated the role of specific sphingomyelinase enzyme in eliciting the apoptotic effect induced by 8a and 8b in H1299 and H1299 p53+/+ cells. To determine whether inhibition sphingomyelinase activity inhibits the ability of 8a and 8b to induce cytotoxicity in H1299 and H1299 p53 +/+ cells, specific inhibitors of neutral sphingomyelinase (GW4869 15 μM) and acid sphingomyelinase (Desipramine 10 μM) were used. SMase activity assays were performed to verify that the concentration of inhibitor used inhibited the induction of SMase by 8a and 8b treatment (Figure 2A). In H1299 cells treated with 8a, both inhibitors reduced the enzyme activity by more than 90% as measured by the fluorescence intensity produced by the enzymatic reaction while in 8b-treated cells, neutral SMase inhibitor had a better effect in reducing the enzyme activity by more than 80% but acid inhibitor reduced the activity by less than 40% (Figure 2A). In cells over-expressing p53, desipramine, the acid SMase inhibitor, reduced >70% of the enzyme activity in 8a-treated cells and in 8b-treated cells neutral SMase inhibitor had a similar reduction of more than 60% of the activity (Figure 2A). In keeping with the SMase inhibitor activity analysis, the cell viability experiments revealed that in H1299 cells treated with 8a, both inhibitors altered the cell viability of treated cells but a more significant effect ($p<0.01$) was observed with the neutral SMase inhibitor treated cells. In 8b treated H1299 cells, GW4869 significantly abrogated the ability of 8b to reduce cell viability but desipramine had no effect as compared to the cells treated with 8b alone (Figure 2B). In H1299 p53 +/+ cells treated with 8a, desipramine had a significantly ($p<0.05$) better effect in inhibiting 8a anti-cancer effect. While in 8b treated H1299 p53 +/+ cells, GW4869 significantly ($p<0.05$) abrogated 8b's anti-cancer effect (Figure 2B). These results taken together suggest that acid and neutral sphingomyelinase activity are required for 8a to illicit its anti-cancer effect while mainly neutral sphingomyelinase is required for 8b-induced cytotoxicity. We next examined the effect of 8a and 8b on ceramide generation. First we studied ceramide production in treated H1299 and H1299 p53+/+ cells using flow analysis (Figure 2C) and then to evaluate whether the ceramide generated is due to de novo synthesis, H1299 and H1299 p53+/+ cells were treated with/without 50 μM fumonisin B1, a potent ceramide synthase inhibitor and with/without 100 μM of 8a and 8b or left untreated for 24 h. The cell viability assays with fumonisin B1 inhibitor revealed that they followed a similar trend to cells treated with 8a and 8b alone (Figure 2D) suggesting that ceramide production in cells treated with 8a and 8b is through the sphingomyelinase pathway.

Gene expression profiling of lung cancer cells treated with 8a and 8b. For a small scale and focused analysis of gene expression upon treatment of 8a and 8b in H1299 and H1299 p53+/+ cells, we used SABiosciences apoptosis array kit to study 84 genes involved in apoptosis that were regulated by the treatment compared to the untreated control. In the current study only those genes that had >2-fold change and were significantly ($p<0.05$) up- or down-regulated compared to the untreated control were included (Tables I-IV). After 24 h treatment of H1299 cells with 8a, expression of 4 genes involved in apoptosis were changed compared to the untreated control. Pro-apoptotic genes, *caspase 4* (involved in Fas mediated apoptosis) and *TNFRSF9* (receptor belonging to the tumor necrosis factor superfamily) were up-regulated (Table I). Previous studies have demonstrated that myeloid cell leukemia sequence 1, *mcl-1*, gene is over expressed in NSCLC (10), but in H1299 cells treated with 8a mcl-1 gene expression was down regulated as compared to the untreated control. Also, X-linked inhibitor of apoptosis, XIAP gene, was down regulated (Table I). In H1299 p53 +/+ cells 8a induces the over expression of death domain family of genes FADD and especially TRADD (fold change of >200) which are recruited by death receptors to transmit the apoptosis signal within the cell from the plasma membrane (Table II). *APAF-1* gene that is essential for mitochondrial apoptosis signaling was also up-regulated with the treatment (Table III). Along with the up-regulation of pro-apoptosis transducers, in 8a-treated H1299 p53+/+ cells there was down-regulation of bcl-2, an inhibitor of the mitochondrial pathway and Gadd45a, an important marker used for the prognosis of NSCLC (Table II). Bcl-2 family of genes includes both inhibitors and facilitators of apoptosis. In H1299 cells, 8b induces over expression of apoptosis-promoting genes, primarily those involved in TNF death receptor apoptosis signaling including *TNF, TNFSF8, card6, TRAF4* and more significantly *TRAF2* (Table III). 8b also induces HRK gene expression, which is a known inhibitor of bcl-2 and LTBR gene expression, a plasma membrane receptor that triggers apoptosis when activated. Also, over-expression of 2 anti-apoptosis genes, *XIAP*, an inhibitor of apoptosis, and *IGF1R* gene that is involved in promoting tumorigenesis, occurred with the treatment of 8b in H1299

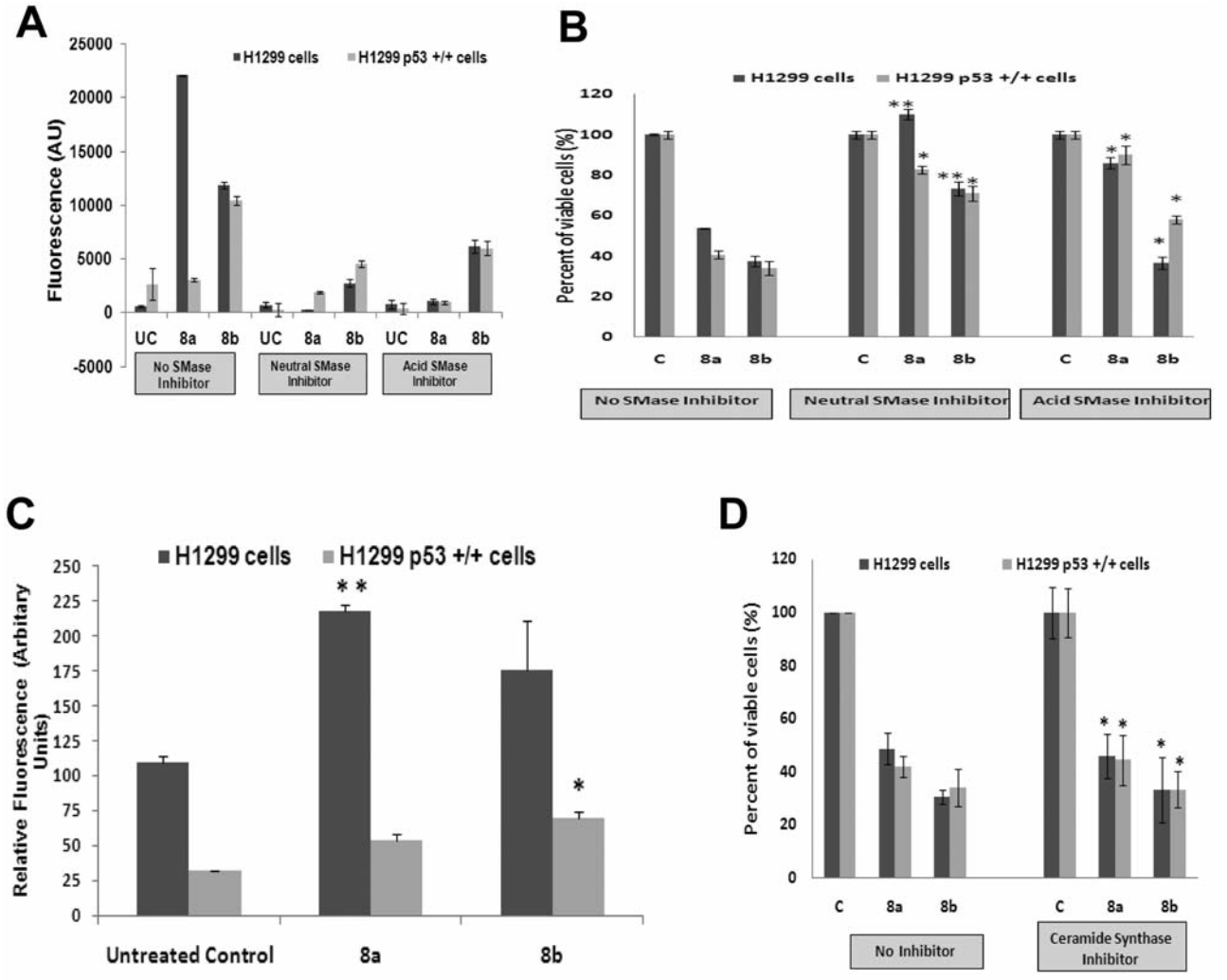

Figure 2. *8a or 8b induce apoptosis of lung cancer cells through activation of sphingomyelinase pathway via ceramide production. H1299 and H1299 p53 +/+ cells were treated with or without (No Smase Inhibitor), Neutral Smase (GW4869 15 μM), or Acid Smase (Desipramine 10 μM) inhibitors for 1 hr before treating the cells with 100 μM 8a or 8b or left untreated (UC/C) for 24 hr. (A) Cell were analyzed for SMase activity as described in Materials and Methods. The histogram represents mean fluorescence (+ SD) measured at 560/590 nm (excitation/emission) of triplicate measurement. (B) The number of viable cells after treatment was determined using MTT assay as described in Materials and Methods. The histogram represents percentage of viable cells (+ SD) normalized using untreated control. The results are indicative of 3 independent experiments. Significance as compared to the treatment without inhibitor was * $p < 0.05$ and ** $p < 0.01$. H1299 and H1299 p53 +/+ cells were treated with or without (Untreated Control) 100 μM 8a or 8b for 24 hr and assayed for ceramide production using (C) flow cytometry by using FITC-labeled mouse monoclonal anti-CER15B4. The histogram represents mean fluorescence (+ SD) subtracting Isotype control fluorescence of 3 independent experiments done in triplicate. Significance as compared to untreated control was * $p < 0.05$ and ** $p < 0.01$. (D) The number of viable cells after treatment was determined using MTT assay as described in Materials and Methods. The histogram represents percentage of viable cells (+ SD) normalized using untreated control. The results are indicative of 3 independent experiments. Significance as compared to the treatment without inhibitor was * $p < 0.05$.*

cells (Table III). In H1299 p53+/+ cells, 8b induces over-expression of bax (bcl-2 associated X protein), *bag 3* (bcl2 associated anthanogene 3), *bcl2l10* (bcl-2 like 10) *bclaf1* (bcl2 associated transcription factor 1), *bik* (bcl-2 interacting killer) and *bnip3l* (bcl-2/adenovirus E1B 19 kDa interacting protein like) genes all known apoptosis facilitators (Table IV) along with the down-regulation of potent inhibitors of apoptosis, *bcl2l1* or *bcl-X* (bcl-2 like 1), *bcl2l2* (bcl-2 like 2) and *mcl-1* genes (Table IV). 8b induces death domain genes expression, *FADD* and TRADD and over-expression of TNF receptor gene, LTBR gene in H1299 p53+/+ cells (Table IV).

Downstream targets of sphingomyelinase-induced apoptosis. Both neutral and acid sphingomyelinase enzymes are activated by death receptors (11) and procaspase 8 is cleaved on activation of death receptors to form activated

Table I. *Fold change of apoptotic gene expression in H1299 cells (null for p53) after 24 h treatment of quinuclidinone derivative 8a, as determined by apoptosis gene array analysis.*

Genes	Fold change Mean±SEM
Up-regulated	
Caspase Family	
Caspase 4 (Caspase 4 apoptosis-related cysteine peptidase)	+2 (±0.01)*
TNF Receptor Family	
TNFRSF9 (Tumor Necrosis Factor Receptor Superfamily, membrane 9)	+3.48 (±0.07)*
Down-regulated	
BCL2 Family	
Mcl-1 (myeloid cell leukaemia sequence 1) BCL2-related	–13.93 (±0.07)*
IAP Family	
XIAP (X-linked inhibitor of apoptosis)	–48.50 (±0.14)*

Fold change is expressed as mean values of the group treated with 100 μM quinuclidinone derivative 8a compared to those of the untreated control group; + indicates gene up-regulation after treatment; - indicates gene down regulation after treatment; *indicates significant gene regulation ($p \leq 0.05$); n=2.

Table II. *Fold change of apoptotic gene expression in H1299 cells p53 +/+ (over expressing p53) after 24 h treatment of quinuclidinone derivative 8a, as determined by apoptosis gene array analysis.*

Genes	Fold change@ Mean±SEM
Up-regulated	
CARDD Family	
APAF-1 (apoptotic peptidase activating factor 1)	+6.73 (±0.9)*
Death Domain Family	
FADD (Fas (TNFRSF6)-associated via death domain)	+6.28 (±0.28)*
TRADD (TNFRSF1A-associated via death domain)	+274 (±0.8)*
Down-regulated	
BCL2 Family	
Bcl 2 (B-cell CLL/lymphoma 2)	–2.93 (±0.9)*
Other	
Gadd45a (Growth arrest and DNA-damage-inducible, alpha)	–2.3 (±0.9)*

Fold change is expressed as mean values of the group treated with 100 μM quinuclidinone derivative 8a compared to those of the untreated control group; + indicates gene up-regulation after treatment; - indicates gene down regulation after treatment; *indicates significant gene regulation ($p \leq 0.05$); n=2.

caspase 8 (12). From gene expression analysis genes involved in TNF receptor pathway were up-regulated by both 8a and 8b. Therefore to examine whether death receptors are involved in 8a and 8b induced cell death, processing of procaspase 8 protein was determined using western blot analysis at different time intervals after treatment with the derivatives 8a or 8b. 8a induced the processing of procaspase 8 as early as 1 h after treatment and significantly by 6 h after treatment in H1299 cells (numbers in between procaspase 8 and GAPDH represent pixel density analysis values normalized to 0 h treatment) (Figure 3A). 8b induction of procaspase 8 processing was similar for both cell lines (Figure 3B). Altogether, these results suggested that in H1299 and H1299 p53+/+ cells, 8a and 8b induced sphingomyelinase activity through the death domain receptors. Moreover, it appeared that 8a and 8b effect was strongest at 24 h after treatment where apoptosis was detected. Downstream targets of sphingomyelinase apoptosis pathway as induced by 8a or 8b treatment of H1299 and H1299 p5+/+ were analyzed using western blotting. Caspase 8 can activate the mitochondrial pathway for apoptosis through key pro-apoptosis proteins, bax and caspase 9. 8a and 8b induced bax expression (Figure 3C/D) with decrease in bcl-2 expression (Figure 3E), release of cytochrome *c* to the cytoplasm from the mitochondria (Figure 4A/B), and increased caspase 9 expression (Figure 4C/D), as demonstrated by western blot analysis.

Discussion

Most chemotherapeutics induce tumor regression by causing apoptosis. Apoptosis, programmed cell death, is conserved sequence of events that is characterized by the formation of nuclear and cytoplasmic blebbing, DNA fragmentation and cell shrinkage (13-16). Apoptosis hallmark is the activation of effector caspases 3 and 7 that is often triggered by either an extrinsic receptor or intrinsic mitochondrial pathway (17, 18). In chemotherapeutic, induced apoptosis these paths are indistinguishable as both are activated due to interplay of molecules boosting the apoptosis signal by the chemical. Previous reports on quinuclidinone derivatives show that they cause apoptosis and cell-cycle arrest in combination with radiation. Here we demonstrated that 8a and 8b are ideal chemotherapeutics and can be used alone to cause apoptosis in human non-small lung cancer cells by activating the neutral sphingomyelinase pathway. Caspase-3 activation is often the beginning of the execution step of apoptosis when the cells become irreversibly committed to cell death (19, 20). It activates DNA degrading enzymes, such as DFF4, and prevents DNA repair proteins, PARP, by cleaving it into inactive forms (21, 22). In our study we see caspase-3 activation with decreased procaspase 3 levels and with

Table III. *Fold change of apoptotic gene expression in H1299 cells (null for p53) after 24 h treatment of quinuclidinone derivative 8b, as determined by apoptosis gene array analysis.*

Genes	Fold change@ Mean±SEM
Up-regulated	
BCL2 Family	
HRK (Harakiri, BCL2 interacting protein (contains only BH3 domain))	+2**
CARDD Family	
Card 6 (Caspase recruitment domain family, member 6)	+2.81 (±0.92)*
IAP Family	
XIAP (X-linked inhibitor of apoptosis)	+2.7 (±0.21)*
TNF Ligand Family	
TNF (Tumor necrosis factor (TNF superfamily, member 2))	+2.43 (±0.92)*
TNFSF8 (Tumor necrosis factor (ligand) superfamily, member 8)	+3.0*
TRAFF Family	
TRAF2 (TNF receptor-associated factor 2)	+2 (±0.5)**
TRAF 4 (TNF receptor-associated factor 4)	+2 (±0.8)*
TNF Family	
LTBR (Lymphotoxin beta receptor or TNFR superfamily, member 3)	+3.1 (±0.8)*
Other	
IGF1R (Insulin-like growth factor 1 receptor)	+2 (±0.14)*

Fold change is expressed as mean values of the group treated with 100 μM quinuclidinone derivative 8b compared to those of the untreated control group; + indicates gene up-regulation after treatment; - indicates gene down regulation after treatment; *indicates significant gene regulation ($p \leq 0.05$); ** indicates significant gene regulation ($p \leq 0.01$); n=3.

Table IV. *Fold change of apoptotic gene expression in H1299 cells p53 +/+ (over expressing p53) after 24 h treatment of quinuclidinone derivative 8b, as determined by apoptosis gene array analysis.*

Genes	Fold change@ Mean±SEM
Up-regulated	
BCL2 Family	
Bag3 (BCL2-associated athanogene 3)	+2.1 (±0.45)*
Bax (BCL 2- associated X protein)	+2.83 (±0.55)*
BclA1 (BCL 2 related protein A1)	+2.96 (±0.18)*
Bcl2l10 (BCL2-like 10) apoptosis facilitator	+2.25 (±0.45)*
Bclaf1 (BCL2-associated transcription factor 1)	+2.05 (±0.7)*
Bik (BCL2-interacting killer) apoptosis-inducing	+2.25 (±0.16)*
Bnip3l (BCL2/adenovirus E1B 19kDa interacting protein 3 like)	+36.76 (±0.9)*
TNF Family	
LTBR (Lymphotoxin beta receptor (TNFR superfamily, member 3))	+3.65 (±0.99)**
Death Domain Family	
FADD (Fas (TNFRSF6)-associated via death domain)	+9.2 (±0.55)*
TRADD (TNFRSF1A-associated via death domain)	+660 (±0.75)*
Down-regulated	
BCL2 Family	
Bcl2l1 (BCL2 –like 1)	–8 (±0.41)*
Bcl2l2 (BCL2 –like 2)	–4 (±0.93)*
Mcl-1 (myeloid cell leukaemia sequence 1) BCL2-related	–9.62 (±0.97)*

Fold change is expressed as mean values of the group treated with 100 μM quinuclidinone derivative 8b compared to those of the untreated control group; + indicates gene up-regulation after treatment; - indicates gene down regulation after treatment; *indicates significant gene regulation ($p \leq 0.05$); *indicates significant gene regulation ($p \leq 0.01$); n=3.

increased cleavage of PARP-1 when treated with PRIMA-1 derivative 8a and 8b in both lung cancer cell lines, indicating that the mechanism by which the derivative works is apoptosis-independent of p53 status.

Many studies show that cell phase arrest especially S-phase arrest, is notable along with chemotherapeutic-induced apoptosis. Presumably, the S-phase arrest helps anticancer drugs target more cells for apoptosis (23-25). In our analysis, quinuclidinone derivatives 8a and 8b promoted increased apoptosis in lung cancer cell lines at 24 h after treatment, as seen by caspase-3 activity and PARP-1 cleavage. This coincides with the S phase cell-cycle arrest seen with treatment. 8a, which works better in H1299 cells null for p53, showed increased S phase arrest in the same cell line; similarly 8b which works well in H1299 p53+/+ cells showed an increased S phase arrest in these cells. These results suggest that increased S phase arrest does sensitize the cells to chemotherapeutic apoptosis.

Many different pathways may lead to the same chemotherapeutic-induced apoptosis; therefore it becomes pertinent to identify the players involved in the apoptotic process induced by quinuclidinone derivatives. Malki *et al.* in 2011 showed that sphingomyelinase activity increases with formation of ceramide in human lung cancer cells treated with 8a and 8b. We demonstrated for the first time, that each derivative activates different types of sphingomyelinase depending on p53 status of the cells. We characterized SMase activity induced by 8a and 8b using potent neutral and acid sphingomyelinase inhibitors. Evidence from inhibitor studies suggests that both neutral and acid sphingomyelinase were induced by 8a and only neutral sphingomyelinase was induced by 8b in H1299 cells. While in H1299 p53+/+ cells, 8a predominantly induced acid sphingomyelinase and 8b induced neutral sphingomyelinase. These results suggest that SMase is an important upstream regulator for apoptosis induced by 8a and 8b in lung cancer cells and when inhibited, it abolishes the derivatives anti-cancer activity establishing their upstream involvement in cellular response to both 8a and 8b. The difference between

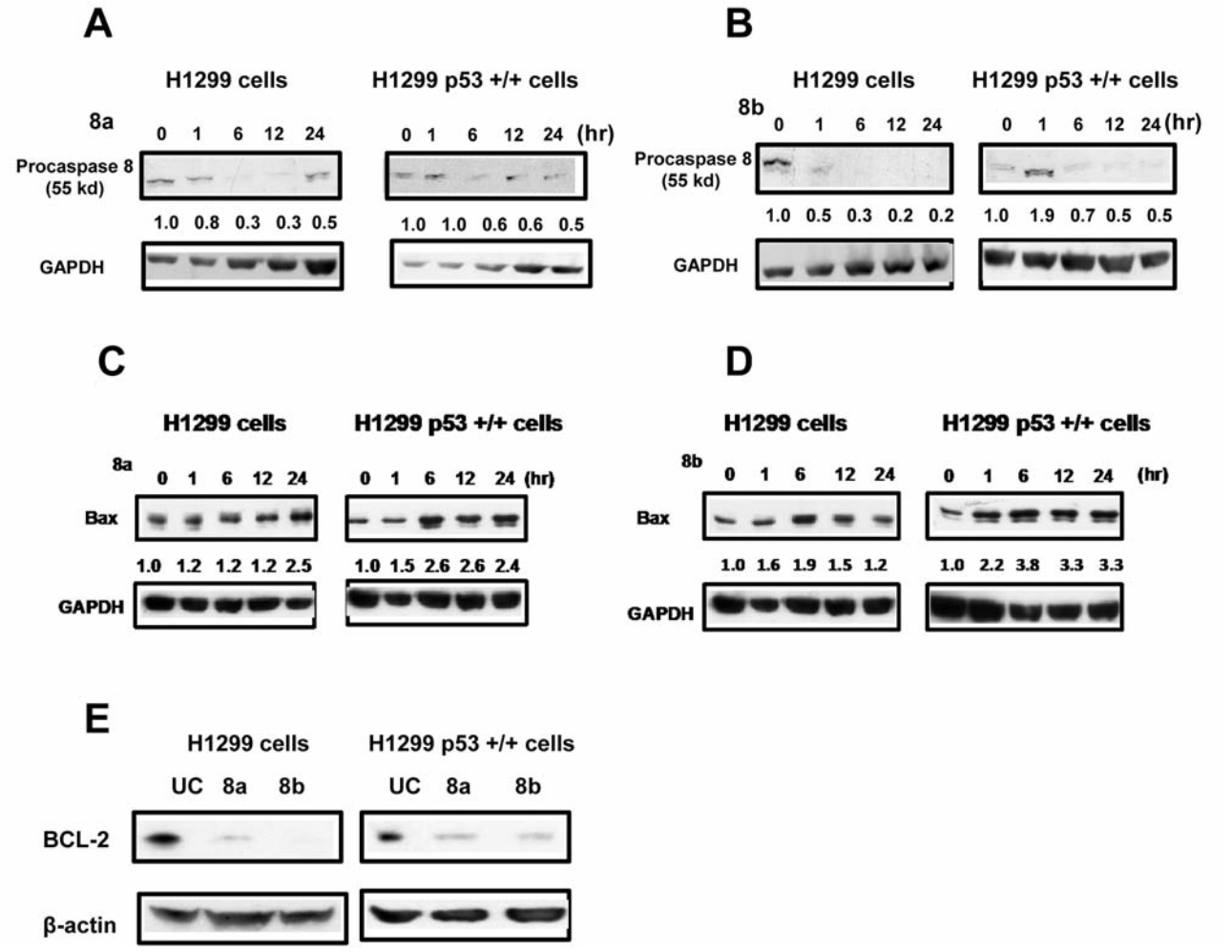

Figure 3. *8a and 8b induce procaspase 8 processing in a time dependent manner and up regulate bax but decrease bcl-2 protein. H1299 and H1299 p53 +/+ cells were treated with 100 μM 8a (A) and 8b (B) for the indicated time intervals and the cell lysate was subjected to western blot analysis to determine procaspase 8 processing using anti-caspase 8 antibody that detects the 55 kDa precursor of caspase 8. The numbers between the procaspase 8 and GAPDH panels indicate fold change in pixel density values of procaspase 8 as compared to its untreated control and normalized to its respective GAPDH pixel density value. Results are representative of 3 independent experiments. H1299 and H1299 p53 +/+ cells were treated with 100 μM 8a (C) or 8b (D) for the indicated time interval and bax protein expression level was determined from whole cell lysates by western blot analysis using mouse monoclonal anti-Bax antibody. GAPDH was used as the loading control. The numbers between the bax and GAPDH panels indicate fold change in pixel density values of bax as compared to its untreated control and normalized to its respective GAPDH pixel density value. Results are representative of 3 independent experiments. (E) H1299 and H1299 p53 +/+ cells were treated with 100 μM 8a, 8b or left untreated (UC) for 24 hr and bcl-2 protein expression level was determined from whole cell lysates by western blot analysis using mouse monoclonal anti-bcl-2 antibody. β-actin was used as the loading control. Results are representative of 3 independent experiments.*

isoforms induction could be related to 8a and 8b triggering different receptors and also due to presence of different p53 status. p53 has been shown to activate neutral sphingomyelinase during oxidative stress (26), which may explain its activation in H1299 p53+/+ cells treated with 8b as previously reported that 8b induces p53 than 8a (8). Ceramide, a hydrolysis product of sphingomyelin generated by both neutral and acid sphingomyelinase and a known second messenger of apoptosis (27-30), was induced in both H1299 and H1299 p53+/+ cells when treated with either 8a or 8b. Ceramide generation correlates with SMase stimulation in both cell lines by 8a and 8b. In H1299 cells, where both N-SMase and A-SMase are induced, there is a higher induction of ceramide production compared to the untreated controls. Similarly in H1299 p53 +/+ cells where 8b stimulates more apoptosis, 8b also induces an increased ceramide generation compared to untreated controls. The *de novo* pathway involving ceramide synthase can also generate

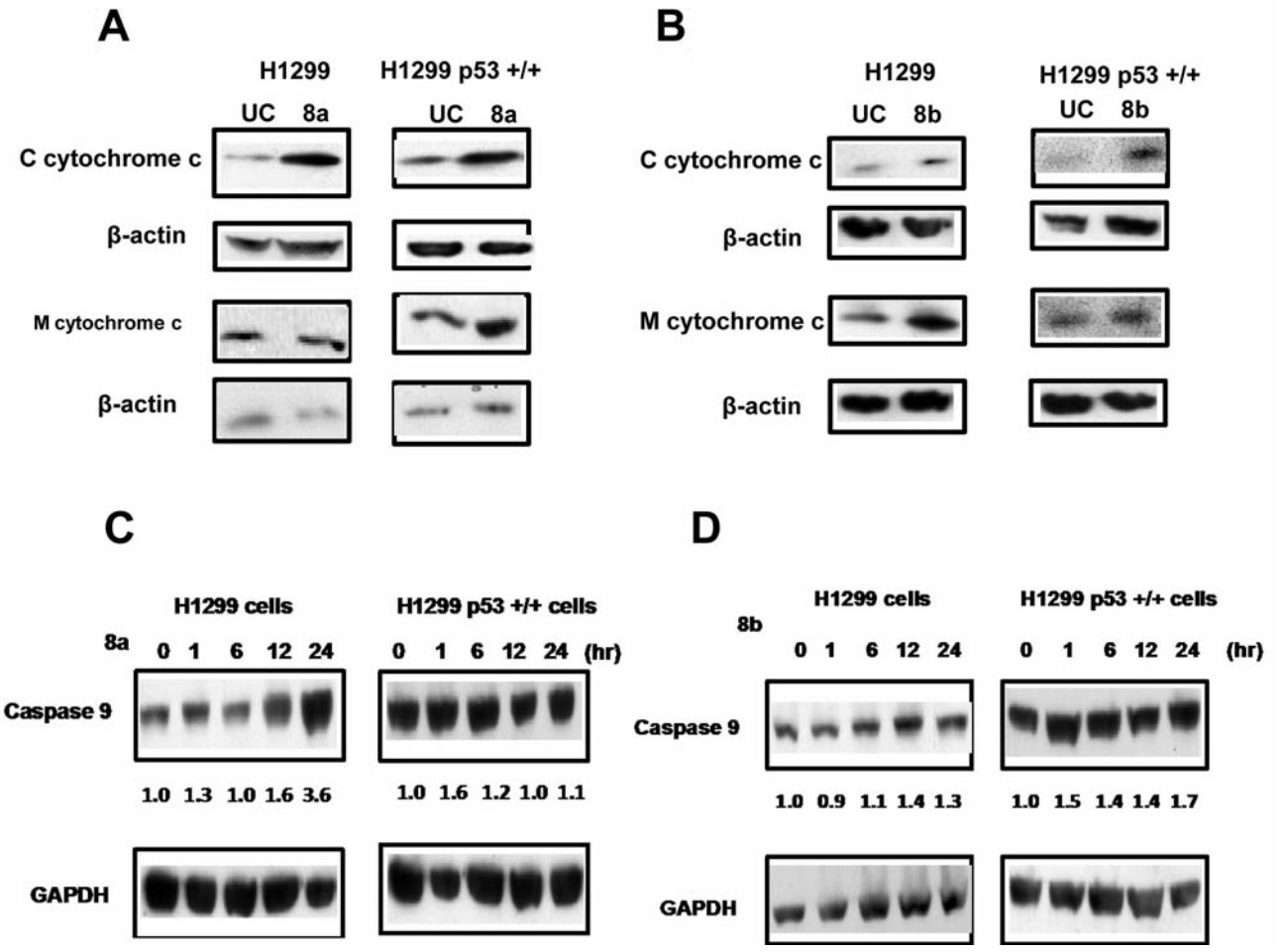

Figure 4. *Downstream activation of mitochondrial apoptosis pathway by 8a an 8b treatment of lung cancer cells. H1299 and H1299 p53 +/+ cells were treated with (+) or without (-) 100 μM 8a (A) or 8b (B) for 24 hr then mitochondrial and cytosolic fractions were separated as described in Materials and Methods. Cytochrome c expression in each fraction was determined by western blot analysis using mouse monoclonal anti-cytochrome c antibody. β-actin was used as the loading control. Results are representative of 3 independent experiments. 'C Cytochrome c' represents cytosolic cytochrome c and 'M Cytochrome c' represents mitochondrial cytochrome c. H1299 and H1299 p53 +/+ cells were treated with 100 μM 8a (C) or 8b (D) for the indicated time interval and caspase 9 protein expression level was determined from whole cell lysates by western blot analysis using mouse monoclonal anti-caspase 9 p10 antibody that detects the caspase 9 cleaved fragment. GAPDH was used as the loading control. The numbers between the caspase 9 and GAPDH panels indicate fold change in pixel density values of caspase 9 as compared to its untreated control and normalized to its respective GAPDH pixel density value. Results are representative of 2 independent experiments.*

cellular ceramide (27-29, 31). There is no role of de novo synthesis of ceramide in the cellular response of 8a and 8b induced apoptosis as seen by the inhibition of ceramide synthase having no effect on 8a and 8b anti-cancer activity.

After understanding that sphingomyelinase is required for both 8a and 8b molecular mechanism, the next goal was to identify differences or similarities in gene expression pattern associated with these novel derivatives. The gene expression profiling for 8a in NSCLC revealed a different pattern with changing p53 status. In 8a treated H1299 cells there was up-regulation of caspase 4 expression that is involved in Fas mediated apoptosis and TNF receptor super family 9 (TNFRSF9 also known as CD137 or 4-1BB) expression. TNFRSF9 is a tumor suppressor marker identified for NSCLC (32) and is an inducible target recognized for anti-tumor immune response, therefore being investigated for immunotherapy (33, 34) Here, the results obtained suggest that 8a can be used as an adjuvant for immunotherapy. Along with up-regulation of pro-apoptotic genes, 8a also down regulated key anti-apoptotic genes, mcl-1and XIAP. Mcl-1 belongs to the bcl-2 family and is involved in inhibiting apoptosis by interacting with pro-apoptotic proteins such as

bak (35). In contrast to reports where *mcl-1* overexpression in NSCLC may be affecting chemosensitivity (10), 8a down-regulates the gene. XIAP, also a potent inhibitor of apoptosis that binds to caspases 3, 7 and 9 and prevents their activity (36), is critical for chemosensitivity. Therefore in NSCLC, inhibitors of XIAP are used in conjunction with known chemotherapy to increase its effectiveness (37). Here, 8a significantly decreases XIAP gene expression by almost 50-fold in H1299 cells. 8a regulates a different set of genes in cells over-expressing p53. Herein, the results indicate that the death domain genes, *TRADD* and *FADD*, were up-regulated, especially *TRADD* (>200-fold). The over expression of these genes induces acid sphingomyelinase activity through the TNF receptor (38). We showed that 8a induces acid sphingomyelinase activity in H1299 p53+/+ cells, which correlates with increased expression of TRADD and FADD. TRADD transcriptional activation causes apoptosis independent of p53 (39); therefore, our results suggest 8a may induce initially a p53-independent apoptosis pathway through the activation of acid sphingomyelinase. 8a treatment leads to an up-regulation of APAF-1, transcriptional target of p53, by the treatment of 8a in the H1299 p53 +/+ cells. APAF-1 binds to cytochrome *c* and recruits procaspase 9 forming an apopotosome that is an essential functional unit for mitochondrial apoptosis to occur (40). Up-regulation of APAF-1, increase release of cytochrome *c*, and presence of caspase 9 all suggests the mitochondrial pathway is involved in 8a induced apoptosis and is p53-dependent in H1299 p53+/+ cells. Interestingly, Gadd45a also a p53 transcription target is down-regulated in these cells with the treatment. However, here the down regulation of Gadd45a could be related to 8a's lower effect in these cells compared to H1299 cells and may be p53-independent. Similar to 8a, 8b also regulates different genes in cells with different p53 status. In H1299 cells that are null for p53, 8b induces mostly genes (*TNF*, *TNFSF8*, *TRAF2*, *TRAF4*, *LTBR*) involved in TNF receptor apoptosis signaling (41-44). Interestingly, in these cells 8b triggers neutral sphingomyelinase that is mainly induced due to the activation of TNF receptor therefore laying a premise for this particular gene regulation observed with 8b treatment. Among extracellular death receptor signaling genes, HRK (*DP5*), a gene identified in regulating intracellular mitochondrial pathway, was up-regulated with 8b treatment. HRK interacts with bcl-2 and bcl-xL through the BH3 domain thereby preventing their inhibitory activity (45). Interestingly, two genes known to inhibit apoptosis, *XIAP* and *IGF1R*, were also induced by 8b treatment in H1299 cells, (37, 46, 47) thus may contribute towards the lowered effect of the derivative in H1299 cells. In H1299 p53+/+ cells, 8b induces the up-regulation of bcl-2 family of genes that are pro-apoptotic (*bag3, bax, bcla1, bcl2l10, bclaf1, bik* and *bnip3l*) and down-regulates those that are anti-apoptotic (*bcl2l1, bcl2l2* and *mcl-1*) (48). Bax expression pattern in the array analysis was consistent with the western blot analysis presented in this study. This opposing regulation changes the balance between pro- and anti-apoptotic proteins leading to increased apoptosis in these cells. Bcl-2-related proteins are mainly involved in mitochondrial apoptosis. Thus, from the bax, cytochrome *c* and caspase 9 results along with the array analysis results, a very important role is suggested for mitochondrial apoptosis in 8b mediated apoptosis in NSCLC cells over-expressing p53. Interestingly, similar to 8a, 8b also induces high expression of TRADD and FADD in H1299 p53+/+ cells. These results taken together suggest that a common receptor may be involved in eliciting 8a and 8b activity in H1299 p53+/+ cells, such as the TNF receptor, being that TRADD expression is significantly higher than FADD expression. It is also plausible that p53 is involved in the transcriptional activation of these genes, although this has not been shown before therefore would need further assessment to define this role. 8b activated neutral sphingomyelinase in both cell types and also induced up-regulation of TNFRSF3 (or LTBR) suggesting that TNF receptor is possibly the predominant receptor involved in 8b activity in these cells.

Many studies indicate that when death receptors, such as TNF-α, Fas and TRAIL, are involved, procaspase 8 is cleaved to form active caspase 8 which either activates effector caspase 3 directly or triggers the mitochondrial apoptosis pathway through the BCL-2 related family members (49). Ceramide amplifies the death receptor apoptotic signals by forming platforms to cluster the receptors through the activation of sphingomyelinase (27, 50-52). In our study, by the formation of caspase 8 after drug treatment in lung cancer cells, confirms the involvement of death receptors as seen with gene expression analysis and maybe mediated through sphingomyelinase activation and formation of ceramide.

Interestingly, for mitochondrial apoptosis pathway to be triggered, bax levels often increase so that it may bind to the outer mitochondrial membrane to allow the release of cytochrome *c*. Bax function is inhibited by BCl-2, that binds to bax and prevents it from binding to the mitochondrial membrane (53-55). We report here that bax levels increased at the same time as bcl-2 levels, that decreased with the treatment of derivative 8a and 8b presumably disrupting the balance between pro- and anti- apoptotic proteins, which would further promote the apoptosis signal. Cytochrome *c* in the cytoplasm forms the apopotosome complex that causes the cleavage of procaspase 9 to caspase 9. Caspase 9 is an important molecule in mitochondrial-triggered apoptosis causing the activation of caspase 3, an effector caspase marking the key last step of apoptosis (40, 56, 57). With the increase in bax protein levels, an increase in caspase 9 levels would be crucial to suggest the mitochondrial apoptosis

pathway involvement. As observed with the treatment of quinuclidinone derivative 8a and 8b in both H1299 and H1299 p53+/+ cells, bax levels increased with an increase in caspase 9 levels. Although chemotherapeutics activate the receptor death pathway, the mitochondria-mediated anti-cancer drug death pathway is also essential. Herein we suggest not only the initial activation through the death receptors, but also an active involvement of the mitochondria in mediating apoptosis by the novel anti-cancer drug quinuclidinone derivatives 8a and 8b.

Overall, our findings suggest that quinuclidinone derivatives 8a and 8b induced apoptosis in H1299 and H1299 p53+/+ cells along with S-phase arrest. Our data suggest that the sphingomyelinase-mediated apoptosis predominantly involves the TNF receptor super-family, as seen by the various results that show different SMase isoform activation depending on the cell type and stimulating derivative. However, the difference in upstream activation gives rise to changes in common downstream effectors involved such as ceramide, caspase 8, bax and bcl-2. Mitochondrial apoptosis-related regulators were involved especially in cells over-expressing p53. These derivatives can work independently of p53 activity but the presence of p53 augments the apoptosis effect. Thus, we are faced with potential novel anticancer drugs that may work through the TNF receptor-sphingomyelinase pathway independent of p53 to induce cellular death of cancer cells initiating a path for target-based drug development.

Acknowledgements

We thank Dr. Stephen Bergmeier's Laboratory for providing the quinuclidinone derivatives used in the study, Dr. Yan Liu for his valuable insights. This work was part of a Ph.D. dissertation of Dr. Eroica Soans, who has obtained permission to cite her own work in this paper (58). The research was partly funded by Early Stage Development Money (ESDM). The authors of this study have no conflict of interest.

References

1 Bykov VJ, Issaeva N, Selivanova G and Wiman KG: Mutant p53-dependent growth suppression distinguishes PRIMA-1 from known anticancer drugs: a statistical analysis of information in the National Cancer Institute database. Carcinogenesis *23*: 2011-8, 2002.

2 Bykov VJ, Issaeva N, Shilov A, Hultcrantz M, Pugacheva E, Chumakov P *et al*: Restoration of the tumor suppressor function to mutant p53 by a low-molecular-weight compound. Nature medicine *8*: 282-8, 2002.

3 Cho Y, Gorina S, Jeffrey PD and Pavletich NP: Crystal structure of a p53 tumor suppressor-DNA complex: understanding tumorigenic mutations. Science *265*: 346-55, 1994.

4 Lambert JM, Gorzov P, Veprintsev DB, Soderqvist M, Segerback D, Bergman J *et al*: PRIMA-1 reactivates mutant p53 by covalent binding to the core domain. Cancer cell *15*: 376-88, 2009.

5 Wang T, Lee K, Rehman A and Daoud SS: PRIMA-1 induces apoptosis by inhibiting JNK signaling but promoting the activation of Bax. Biochemical and biophysical research communications *352*: 203-12, 2007.

6 Li Y, Mao Y, Brandt-Rauf PW, Williams AC and Fine RL: Selective induction of apoptosis in mutant p53 premalignant and malignant cancer cells by PRIMA-1 through the c-Jun-NH2-kinase pathway. Molecular cancer therapeutics *4*: 901-9, 2005.

7 Malki A, Pulipaka AB, Evans SC and Bergmeier SC: Structure-activity studies of quinuclidinone analogs as anti-proliferative agents in lung cancer cell lines. Bioorg Med Chem Lett *16*: 1156-9, 2006.

8 Malki A and Bergmeier S: Differential apoptotic effects of novel quinuclidinone analogs 8a and 8b in normal and lung cancer cell lines. Anticancer Res *31*: 1345-1357, 2011.

9 Sax JK, Fei P, Murphy ME, Bernhard E, Korsmeyer SJ and El-Deiry WS: BID regulation by p53 contributes to chemosensitivity. Nature Cell Biol *4*: 842-849, 2002.

10 Song L, Coppola D, Livingston S, Cress D and Haura EB: Mcl-1 regulates survival and sensitivity to diverse apoptotic stimuli in human non-small cell lung cancer cells. Cancer Biology & Therapy *4*: 267-276, 2005.

11 Marchesini N and Hannun YA: Acid and neutral sphingomyelinases: roles and mechanisms of regulation. Biochemistry and cell biology = Biochimie et biologie cellulaire *82*: 27-44, 2004.

12 Martin DA, Siegel RM, Zheng L and Lenardo MJ: Membrane oligomerization and cleavage activates the caspase-8 (FLICE/MACHalpha1) death signal. The Journal of Biological Chemistry *273*: 4345-4349, 1998.

13 Makin G and Hickman JA: Apoptosis and cancer chemotherapy. Cell Tissue Res *301*: 143-152, 2000.

14 Hengartner MO: The biochemistry of apoptosis. Nature *407*: 770-776, 2000.

15 Fulda S and Debatin KM: Targeting apoptosis pathways in cancer therapy. Curr Cancer Drug Targets *4*: 569-576, 2004.

16 Fulda S and Debatin KM: Modulation of apoptosis signaling for cancer therapy. Arch Immunol Ther Exp (Warsz) *54*: 173-175, 2006.

17 Fulda S and Debatin KM: Extrinsic versus intrinsic apoptosis pathways in anticancer chemotherapy. Oncogene *25*: 4798-4811, 2006.

18 Fulda S and Debatin KM: Apoptosis signaling in tumor therapy. Ann NY Acad Sci *1028*: 150-156, 2004.

19 Rich T, Watson CJ and Wyllie A: Apoptosis: the germs of death. Nat Cell Biol *1*: E69-71, 1999.

20 Green DR: Apoptotic pathways: paper wraps stone blunts scissors. Cell *102*: 1-4, 2000.

21 Oliver L and Vallette FM: The role of caspases in cell death and differentiation. Drug Resist Updat *8*: 163-170, 2005.

22 Fischer U, Janicke RU and Schulze-Osthoff K: Many cuts to ruin: a comprehensive update of caspase substrates. Cell Death Differ *10*: 76-100, 2003.

23 Fulda S and Debatin KM: Sensitization for anticancer drug-induced apoptosis by the chemopreventive agent resveratrol. Oncogene *23*: 6702-6711, 2004.

24 Pucci B, Kasten M and Giordano A: Cell cycle and apoptosis. Neoplasia *2*: 291-299, 2000.

25 Smith DM, Gao G, Zhang X, Wang G and Dou QP: Regulation of tumor cell apoptotic sensitivity during the cell cycle (Review). Int J Mol Med *6*: 503-507, 2000.

26 Sawada M, Nakashima S, Kiyono T, Nakagawa M, Yamada J, Yamakawa H *et al*: p53 regulates ceramide formation by neutral sphingomyelinase through reactive oxygen species in human glioma cells. Oncogene *20*: 1368-1378, 2001.
27 Carpinteiro A, Dumitru C, Schenck M and Gulbins E: Ceramide-induced cell death in malignant cells. Cancer letters *264*: 1-10, 2008.
28 Kolesnick RN and Kronke M: Regulation of ceramide production and apoptosis. Annual review of physiology *60*: 643-665, 1998.
29 Obeid LM and Hannun YA: Ceramide: a stress signal and mediator of growth suppression and apoptosis. Journal of cellular biochemistry *58*: 191-198, 1995.
30 Jarvis WD, Grant S and Kolesnick RN: Ceramide and the induction of apoptosis. Clinical cancer research: an official journal of the American Association for Cancer Res *2*: 1-6, 1996.
31 Spiegel S, Foster D and Kolesnick R: Signal transduction through lipid second messengers. Current Opinion in Cell Biology *8*: 159-167, 1996.
32 Zborovskaia IB and Tatosian AG: Molecular markers of various stages of nonsmall cell lung cancer development. Molekuliarnaia Biologiia *38*: 191-202, 2004.
33 Houot R, Goldstein MJ, Kohrt HE, Myklebust JH, Alizadeh AA, Lin JT *et al*: Therapeutic effect of CD137 immunomodulation in lymphoma and its enhancement by Treg depletion. Blood *114*: 3431-3438, 2009.
34 Sica G and Chen L: Biochemical and immunological characteristics of 4-1BB (CD137) receptor and ligand and potential applications in cancer therapy. Archivum immunologiae et therapiae experimentalis *47*: 275-279, 1999.
35 Leu JI, Dumont P, Hafey M, Murphy ME and George DL: Mitochondrial p53 activates Bak and causes disruption of a Bak-Mcl1 complex. Nature Cell Biology *6*: 443-450, 2004.
36 Deveraux QL and Reed JC: IAP family proteins – suppressors of apoptosis. Genes & Development *13*: 239-252, 1999.
37 Cheng YJ, Jiang HS, Hsu SL, Lin LC, Wu CL, Ghanta VK *et al*: XIAP-mediated protection of H460 lung cancer cells against cisplatin. European J Pharmacology *627*: 75-84, 2010.
38 Schwandner R, Wiegmann K, Bernardo K, Kreder D and Kronke M: TNF receptor death domain-associated proteins TRADD and FADD signal activation of acid sphingomyelinase. The Journal of biological chemistry *273*: 5916-5922, 1998.
39 Yount GL, Afshar G, Ries S, Korn M, Shalev N, Basila D *et al*: Transcriptional activation of TRADD mediates p53-independent radiation-induced apoptosis of glioma cells. Oncogene *20*: 2826-2835, 2001.
40 Li P, Nijhawan D, Budihardjo I, Srinivasula SM, Ahmad M, Alnemri ES *et al*: Cytochrome c and dATP-dependent formation of Apaf-1/caspase-9 complex initiates an apoptotic protease cascade. Cell *91*: 479-489, 1997.
41 Gaur U and Aggarwal BB: Regulation of proliferation, survival and apoptosis by members of the TNF superfamily. Biochemical Pharmacology *66*: 1403-1408, 2003.
42 Hsu H, Shu HB, Pan MG and Goeddel DV: TRADD-TRAF2 and TRADD-FADD interactions define two distinct TNF receptor 1 signal transduction pathways. Cell *84*: 299-308, 1996.
43 Kuai J, Nickbarg E, Wooters J, Qiu Y, Wang J and Lin LL: Endogenous association of TRAF2, TRAF3, cIAP1, and Smac with lymphotoxin beta receptor reveals a novel mechanism of apoptosis. The Journal of Biological Chemistry *278*: 14363-14369, 2003.
44 VanArsdale TL, VanArsdale SL, Force WR, Walter BN, Mosialos G, Kieff E *et al*: Lymphotoxin-beta receptor signaling complex: role of tumor necrosis factor receptor-associated factor 3 recruitment in cell death and activation of nuclear factor kappaB. Proceedings of the National Academy of Sciences USA *94*: 2460-2465, 1997.
45 Imaizumi K, Morihara T, Mori Y, Katayama T, Tsuda M, Furuyama T *et al*: The cell death-promoting gene DP5, which interacts with the BCL2 family, is induced during neuronal apoptosis following exposure to amyloid beta protein. The Journal of Biological Chemistry *274*: 7975-7981, 1999.
46 Dean EJ, Ward T, Pinilla C, Houghten R, Welsh K, Makin G *et al*: A small molecule inhibitor of XIAP induces apoptosis and synergises with vinorelbine and cisplatin in NSCLC. British J Cancer *102*: 97-103, 2010.
47 Riedemann J, Macaulay VM: IGF1R signalling and its inhibition. Endocrine-related Cancer *13*: S33-43, 2006.
48 Adams JM and Cory S: The Bcl-2 protein family: arbiters of cell survival. Science *281*: 1322-1326, 1998.
49 Budihardjo I, Oliver H, Lutter M, Luo X and Wang X: Biochemical pathways of caspase activation during apoptosis. Annu Rev Cell Dev Biol *15*: 269-290, 1999.
50 Grassme H, Schwarz H and Gulbins E: Molecular mechanisms of ceramide-mediated CD95 clustering. Biochem Biophys Res Commun *284*: 1016-1030, 2001.
51 Grassme H, Jekle A, Riehle A, Schwarz H, Berger J, Sandhoff K *et al*: CD95 signaling via ceramide-rich membrane rafts. J Biol Chem *276*: 20589-20596, 2001.
52 Grassme H, Jendrossek V, Bock J, Riehle A and Gulbins E: Ceramide-rich membrane rafts mediate CD40 clustering. J Immunol *168*: 298-307, 2002.
53 Gross A, Jockel J, Wei MC and Korsmeyer SJ: Enforced dimerization of BAX results in its translocation, mitochondrial dysfunction and apoptosis. Embo J *17*: 3878-3885, 1998.
54 Oltvai ZN, Milliman CL and Korsmeyer SJ: Bcl-2 heterodimerizes *in vivo* with a conserved homolog, Bax, that accelerates programmed cell death. Cell *74*: 609-619, 1993.
55 Wolter KG, Hsu YT, Smith CL, Nechushtan A, Xi XG and Youle RJ: Movement of Bax from the cytosol to mitochondria during apoptosis. J Cell Biol *139*: 1281-1292, 1997.
56 Pan G, O'Rourke K and Dixit VM: Caspase-9, Bcl-XL, and Apaf-1 form a ternary complex. J Biol Chem *273*: 5841-5845, 1998.
57 Barinaga M: Death by dozens of cuts. Science *280*: 32-34, 1998.
58 Soans E: Investigating the Molecular Mechanism of Novel Quinuclidinone Derivatives in Lung Cancer Cells with Different p53 Status [Electronic Thesis or Dissertation]. OhioLINK Electronic Theses and Dissertations Center: Ohio University; 2010.

Received May 6, 2014
Revised May 28, 2014
Accepted May 29, 2014